FUNDAMENTALS OF ATMOSPHERIC PRESSURE RF MODULATED DBD IN HELIUM

J.-S. BOISVERT[1,2]*, J. MARGOT[1], F. MASSINES[2]

[1] Université de Montréal, Montréal, H3C 1J7, Canada
[2] Laboratoire PROMES-CNRS, Perpignan, 66000, France
*jean-sebastien.boisvert@umonteal.ca

ABSTRACT

An experimental study of dielectric barrier discharge operated under a pulsed radiofrequency (RF) regime is presented. Various systems are compared in atmospheric pressure helium. The effect of different power sources and different matching networks on electrical and optical behaviour of the discharge are compared. Results are analysed according to positive and negative feedback. Furthermore, optical diagnostic shows that the region with the most dissipated energy varies with the power sources and the electrode length. Insights are given on the kind of discharges that would be optimal for thin film coating.

1. INTRODUCTION

Low pressure plasmas are suitable for many industrial processes. However, the need for vacuum systems significantly raises the cost of the overall process and considerably complicates the manipulation of the samples to be treated. A convenient way to avoid these disadvantages is to use atmospheric pressure plasmas. For example, it has been shown that, using a dielectric barrier discharge (DBD) at atmospheric pressure, silicium based solar cells could reach the same efficiency than those treated by the standard low pressure technics [1]. For several applications, the chemical composition of the discharge requires a high degree of homogeneity. An efficient way of achieving such homogeneity is to operate the discharge at high frequency and to modulate the power applied to the plasma [1, 2]. This clearly necessitates a better understanding of the physics governing atmospheric pressure discharges in such conditions.

Typically, in the radiofrequency range the use of dielectric barriers is less common. However, the use of dielectric barriers in a capacitively coupled discharge was shown to be an efficient way to prevent the glow to arc transition for important current density [3, 4]; it also allows a good stability of the discharge.

2. EXPERIMENTAL

Two plasma reactors are used for this experiment. The discharge cell is a dielectric barrier discharge with a gas flow going from the right to the left (see fig. 1). Both reactors are coupled to a RF source; the discharge gap is 2 mm and the electrode lenght in the gas flow direction is 10 mm. The first power system is made of an arbitrary waveform generator (Agilent 33210A) with a broadband power amplifier (Prâna GN 500). It is coupled to the discharge cell via an homemade transformer tuned around 4.23 MHz (plain line in fig. 1).

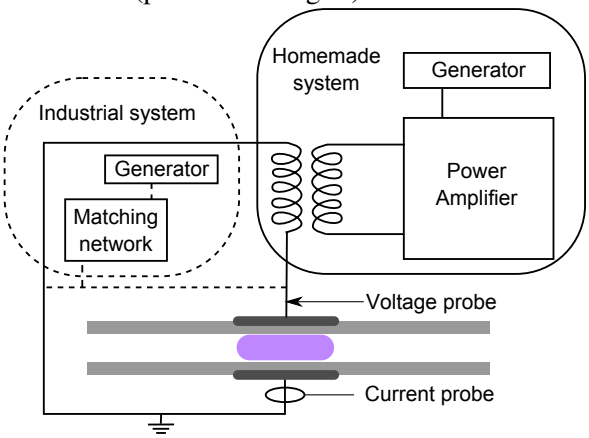

Fig. 1: Simplified scheme of the setups. The gaz is flowing from the right to the left. The length of the electrodes in the flow direction is 0.01 m. Plain line circuit is coupled to the discharge cell by a transformer while the dashed line circuit is coupled by an automatic matching network.

The second one is made of an industrial RF generator (Seren R 601) with an automatic matching network (Seren AT-6). Therefore, the RF generator is coupled to the discharge cell via a "L" net-

work; the generator is fixed at a 13.56 MHz frequency (dashed line in fig. 1). In both cases, current measurement is made via a Rogowski coil on the grounded electrode and voltage measurement is made with an high voltage probe on the high voltage electrode. Imaging and optical emission spectroscopy are made through a quartz window perpendicular to the gas flow (in the largest dimension of the discharge).

3. ELECTRICAL BEHAVIOUR

Using a 5 ms pulse (100 Hz @ 50%) in both generators, different profiles were observed for voltage and current measurements. These profiles are shown in fig. 2. Using the homemade system, while the current and the voltage are oscillating at the radiofrequency, the enveloppe of the profile is increasing gradually until a plateau is reached. On the other hand, for the industrial system, the envelope reaches a maximum and then falls back onto a plateau. It is notable that for an increase of the power, the negative slope is steeper and for a greater gas gap, the difference between the plateau and the maximum of the envelope is greater.

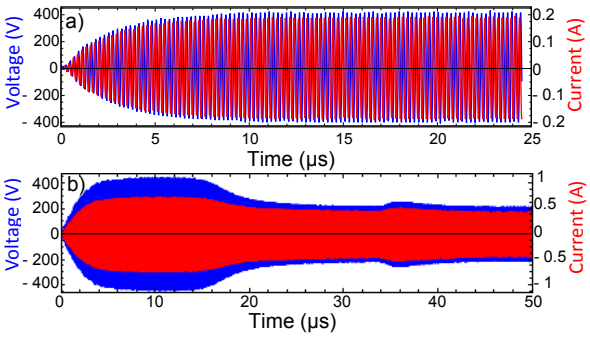

Fig. 2: Voltage and current profiles for a) homemade and b) industrial power systems. The first one shows a positive feedback while the second one shows a negative feedback.

According to Huo et al. [5], the negative slope in the industrial voltage-current profile at around 20 μs is due to a high value of the capacitance in series with the discharge cell. Assuming that

$$P_{injected} \uparrow \Rightarrow \ Area_{disch} \uparrow \Rightarrow C_{pl} \uparrow, \qquad (1)$$

an increase of the plasma capacity can lead to a detuning of the network, thereby decreasing the power of the discharge; whence the negative slope in fig. 2b). Thus, this kind of negative feedback can be usefull for growth of homogeneous thin films since a fast rise of the injected power is beneficial for a fast stabilisation of the chemical species in the gas.

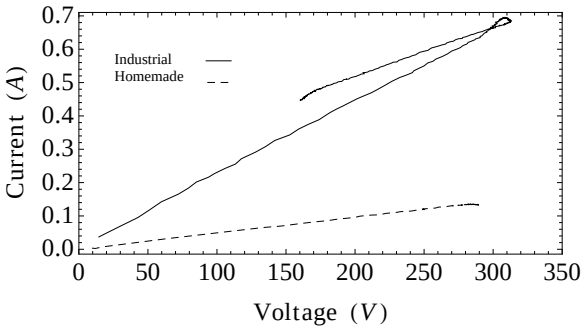

Fig. 3: RMS current-voltage characteristic for both generators. Industrial system is represented by the plain line and the homemade system is represented by the dashed line. The industrial generator curve shows a small negative differential resisitivity region before the drop in power.

During the ignition phase of a pulse, there is an evolution in the RMS values of voltage and current. This evolution can be plotted in the current-voltage characteristic curve of the discharge cell (fig. 3). For the homemade system, the slope of the characteristic is constant while for the industrial system, there is a point at which the power stops and falls back before a stabilisation. At the inflexion, there is a small region of negative differential resistivity. This region can be expanded when the the power at the generator is increased. As in the the characteristic curve of the DC discharge, this region is unstable and can not sustain a steady discharge [6].

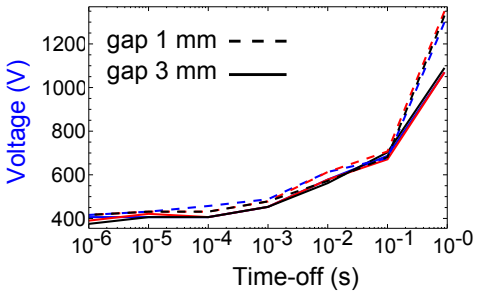

Fig. 4: Maximum voltage vs time-off using the industrial system. Plain lines are for a gas gap of 3 mm while dashed lines are for 1 mm. Measurement for various gas flow between $1.67 \times 10^{-5}\ m^3/s$ and $5.00 \times 10^{-5}\ m^3/s$.

Fig. 4 shows the evolution of the maximum value of voltage during a pulse using the industrial system. Knowing that the current features the same behaviour, it is interesting to note that more power is injected in the discharge for long time-off. This tells us that a long time-off is optimal for injecting a large amount of energy in the gas during the ignition of the plasma which might be useful to rapidly stabilize the chemistry of the discharge.

It is also interesting to note that the voltage does not follow a monotonic evolution when the time-on varies from the millisecond to the second range (unlike voltage evolution with time-off).

4. FAST IMAGING

By injecting more power in the discharge, gas heating can become significant. Overheating might be problematic for the substrate or the discharge dynamics. The use of long time-off modulation is a good way to avoid heating of the gas. Fast imaging of a 5 ms pulse generated by the homemade system is shown in fig. 5. The image shows a serie of pictures taken with a gate width of 1 μs integrated on the discharge length in the gas flow direction.

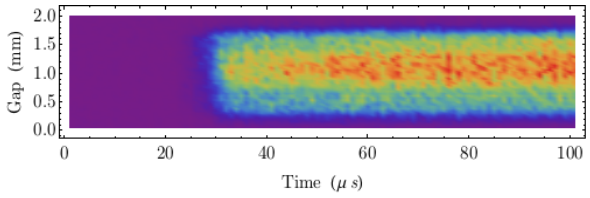

Fig. 5: Evolution of the light emission profile across the gap for 1 μs gate width pictures. This represents the first 100 μs of the discharge ignition for the homemade generator system at low power.

All along the discharge pulse, the light emission intensity is concentrated in the center of the gap. This is typical of the α-mode of a capacitively coupled discharge at atmospheric pressure [7, 8].

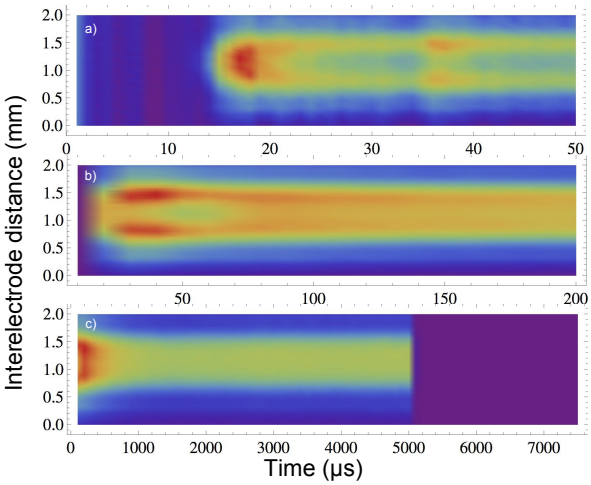

Fig. 6: Evolution of the light emission profile across the gap for a gate width of a) 1 μs, b) 10 μs and c) 100 μs. Pictures where taken for the ignition and the whole pulse. The plasma was generated with the industrial system at low power.

On the other hand, for the industrial system, the resulting imagery is given in fig. 6. During a pulse, the intensity profile shows different discharge behaviours depending on the time scale. In figure 6a), between 10 and 20 μs, the light emission is concentrated in the center, which is typical of the α-mode. The same behaviour is observed in figure 6c) after 1 ms; this is also the time it takes for the discharge to become homogenous in light emission. However, in the 20 μs to $\sim$1 ms interval, the light emission is concentrated closer to the electrodes.

It is interesting to compare the time evolution of the integrated light emission. As it is shown in figure 7, the light emission starts at the maximum of voltage intensity. Hence, it becomes clear that it is the plasma ignition that is producing the voltage drop when the plasma modifies the capacity of the gas gap.

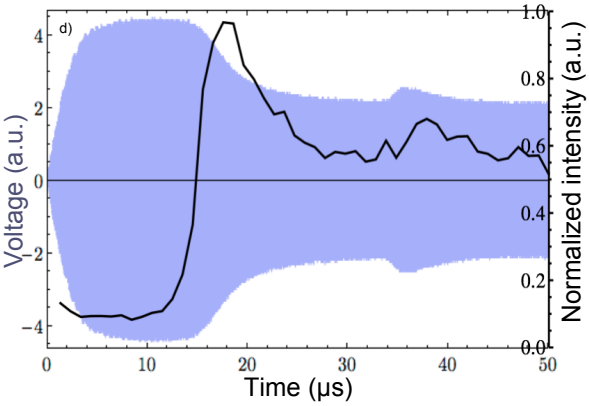

Fig. 7: Correlation of the voltage and maximum integrated light intensity for a pulse generated with the industrial system at low power.

The tuning of the RF network with the discharge cell seems to be the key parameter to control the discharge behaviour. At the μs level, the industrial system transfer a power burst to the plasma leading to a transition in the concentration of light emission. For low power discharge, imagery with a long time integration indicates a concentration of the light emission in the bulk as for the homemade system. In addition, even for the homemade system, it seems possible to concentrate the light emission near the electrode when the frequency is suitably tuned to match the transformer's and the discharge cell's impedance.

5. OPTICAL EMISSION SPECTROSCOPY

Optical emission spectroscopy has also been used to investigate the electrical discharge. Fig. 8 shows three optical emission spectra taken with 20 μs gate width. The lower one corresponds to

the first 20 μs of the discharge while the two others correspond to the 20 subsequent μs. In these spectra, the He line ($^3S \rightarrow {}^3P$) is relatively small compared to most molecular bands. This is due to the high energy level of th $1s3s$ configuration (22.7 eV). This energy level is harder to populate with the low quantity of energetic species discharge ignition. Furthermore, every atomic line grows proportionally between the spectra. However, both OH molecular bands around 300 nm grow faster during the ignition phase. This might be an indication of the presence of long-lived species between two pulses.

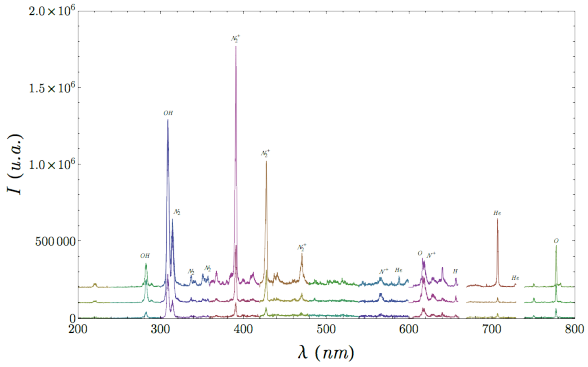

Fig. 8: *Evolution of spectral emission for different times in the discharge. Bottom spectrum is for the first 20 μs of the pulse, middle spectrum is between 20 μs and 40 μs and the top spectrum is between 40 μs and 60 μs (all with 20 μs gate with). These spectra were taken using the industrial system with a 25 ms time-off.*

There is also a continuum in the optical spectral region. This continuum is more prominent with longer gate width and appears with both generator systems. In similar discharges in helium, this have been identify as a bremstralung continuum [9].

6. CONCLUSION

Both power generators, the industrial system with the automatic matching network and the homemade system with the waveform generator and the power amplifier, were proven to be useful to generate pulsed glow discharge with a dielectric barrier discharge in the radiofrequency range. While the homemade system generates a stable glow discharge rapidly reaching a steady state, the industrial system was proven useful to produce a power burst during the ignition and a negative feedback. Optical diagnostic shows that the region with the most dissipated energy can vary along the pulse when using the industrial system.

ACKNOWLEDGMENT

Special thanks go to Institut National de Recherche Scientifique - Énergie Matériaux et télécommunication (Varenne, Québec, Canada) for the time allowed on the plasma reactor.

REFERENCES

[1] J. Vallade, R. Bazinette, L. Gaudy and F. Massines, "Effect of Glow DBD Modulation on Gas and Thin Film Chemical Composition: Case of Ar/SiH_4/NH_3 Mixture", J. Phys. D: Appl. Phys., **47**, 2014

[2] R. Bazinette, J. Vallade, S. Pouliquen, R. Subileau, J. Paillol and F. Massines, "Effect of Frequency excitation on a Homogeneous Dielectric Barrier Discharge At In Ar/NH3 at Atmospheric Pressure", plasmainstitute.org, 2011

[3] S. Y. Moon, W. Choe and B. K. Kang, "A Uniform Glow Discharge Plasma Source at Atmospheric Pressure", Appl. Phys. Let., **84**, 188 – 190, 2004

[4] J. J. Shi, D. W. Liu and M. G. Kong,"Plasma Stability Control Using Dielectric Barriers in Radio-frequency Atmospheric Pressure Glow Discharges", Appl. Phys. Let., **89**, 081502, 2006

[5] W. G. Huo, K. Xu, B. Sun and Z. F. Ding,"Influences of Impedance Matching Network on Pulse-Modulated Radio Frequency Atmospheric Pressure Glow Discharge", Phys. Plasma, **19**, 083502, 2012

[6] Y. P. Raizer, V. I. Kisin and A. E. John *Gas Discharge physics*, Springer-Verlag Berlin, 449, 1991

[7] J. Park, I. Henins, H. W. Herrmann and G. S. Selwyn,"Discharge Phenomena of an Atmospheric Pressure Radio-Frequency Capacitive Plasma Source", J. Appl. Phys., **89**, pp. 20 - 28, 2001

[8] S. Y. Moon, J. K. Rhee, D. B. Kim and W. Choe, "α, γ, and Normal, Abnormal Glow Discharge Modes in Radio-Frequency Capacitively Coupled Discharges at Atmospheric Pressure", Phys. Plasma, **13**, 2006

[9] J. Park, I. Henins, H. W. Herrmann and G. S. Selwyn,"Neutral Bremsstrahlung Measurement in an Atmospheric-Pressure Radio Frequency Discharge", Phys. Plasmas, **7**, pp. 3141 – 3144, 2000